POST PRINT
Pubblicato da Wiley
doi: 10.1002/jcp.26478
URL: https://onlinelibrary.wiley.com/doi/10.1002/jcp.26478

Proteomic expression profile of injured rat peripheral nerves revealed biological networks and processes associated with nerve regeneration

Daniele Vergara[1,2] | Alessandro Romano[3] | Eleonora Stanca[1,2] | Velia La Pesa[3] | Laura Aloisi[3] | Stefania De Domenico[4] | Julien Franck[5] | Ilaria Cicalini[6] | Anna Giudetti[1] | Elisa Storelli[3,7] | Damiana Pieragostino[6] | Isabelle Fournier[5] | Alessandro Sannino[7] | Michel Salzet[5] | Federica Cerri[3] | Angelo Quattrini[3] | Michele Maffia[1,2]

[1] Department of Biological and Environmental Sciences and Technologies, University of Salento, Lecce, Italy

[2] Laboratory of Clinical Proteomic, "Giovanni Paolo II" Hospital, ASL-Lecce, Lecce, Italy

[3] Neuropathology Unit, Institute of Experimental Neurology and Division of Neuroscience, IRCCS San Raffaele Scientific Institute, Milan, Italy

[4] Institute of Sciences of Food Production, National Research Council, Lecce, Italy

[5] Université de Lille, Inserm, U-1192−Laboratoire Protéomique, Réponse Inflammatoire et Spectrométrie de Masse-PRISM, Lille, France

[6] Analitical Biochemistry and Proteomics Unit, Research Center on Aging (Ce.S.I), University "G. d'Annunzio" of Chieti-Pescara, Chieti, Italy

[7] Department of Innovation Engineering, University of Salento, Lecce, Italy

Peripheral nerve regeneration is regulated through the coordinated spatio-temporal activation of multiple cellular pathways. In this work, an integrated proteomics and bioinformatics approach was employed to identify differentially expressed proteins at the injury-site of rat sciatic nerve at 20 days after damage. By a label-free liquid chromatography mass-spectrometry (LC-MS/MS) approach, we identified 201 differentially proteins that were assigned to specific canonical and disease and function pathways. These include proteins involved in cytoskeleton signaling and remodeling, acute phase response, and cellular metabolism. Metabolic proteins were significantly modulated after nerve injury to support a specific metabolic demand. In particular, we identified a group of proteins involved in lipid uptake and lipid storagemetabolism. Immunofluorescent staining for acyl-CoA diacylglycerol acyltransferase 1 (DGAT1) and DAGT2 expression provided evidence for the expression and localization of these two isoforms in Schwann cells at the injury site in the sciatic nerve. This further supports a specific local regulation of lipid metabolism in peripheral nerve after damage.

KEYWORDS
DGAT, LC-MS/MS, lipid metabolism, peripheral nerve injury, proteomics

Correspondance
Michele Maffia, Department of Biological and Environmental Sciences and Technologies, University of Salento, via Monteroni, Lecce, Italy.
Email: michele.maffia@unisalento.it

Funding information
National Operational Programme for Research and Competitiveness (PONREC) "RINOVATIS", Grant number: PON02_00563_3448479; Apulia Regional Cluster project "SISTEMA", Grant number: T7WGSJ3; SIRIC ONCOLille, Grant number: INCa-DGOS-Inserm 6041aa

1 | INTRODUCTION

Peripheral nerve injury is a frequent cause of lasting motor deficits and chronic pain. Although peripheral nerves can regenerate, recovery after axonal damage is sometimes extremely slow and often does not translate into successful functional outcomes. Nerve regeneration in the peripheral nervous system (PNS) requires a coordinated repair response involving the inflammatory system and Schwann cell differentiation and proliferation. Furthermore, this nerve repair process is dependent on a coordinated response between the inductive signals of cytokines, growth factors and the extracellular matrix components (Höke, 2006; Previtali et al., 2008). Following nerve injury, degeneration of the distal stump, referred as Wallerian degeneration, occurs (Stoll, Jander, & Myers, 2002). The process is initiated by elevation of Ca^{2+} influx (Ghosh-Roy, Wu, Goncharov, Jin, & Chisholm, 2010) that activated adenylate cyclase enzymes generating cAMP. The increased cAMP levels with the axonal translation mRNAs and retrograde transport of injury signals are intrinsecal molecular mechanisms to initiate regenerative response mediated by regenera- tion-associated genes (RAGs) (Chandran et al., 2016; Qiu et al., 2002; Twiss, Kalinski, Sachdeva, & Houle, 2016). c-Jun, the first identified RAG (Raivich et al., 2004), and AFT3 are top two hub transcription factors modulating the coordinated expression of many RAGs involved in different pathways (Ma & Willis, 2015; Parikshak, Gandal, & Geschwind, 2015). The relevant downstream signaling pathways seem to be JAK-STAT3, PI3K-Akt, Ras-ERK, and Rho-RKO signaling (Chandran et al., 2016; Chan, Gordon, Zochodne, & Power, 2014; Rishal & Fainzilber, 2014). Besides transcriptional factors, membrane ion channel regulation is also affected after injury (Abe & Cavalli, 2008;Chandran et al., 2016).

Schwann cells represent a key player in nerve repair, they are implicated in myelin degradation, inflammatory response, debris removal, and upregulation of neurotrophic and neuritogenic factors supporting axon sprouting and outgrowth (Höke, 2006; Jessen, Mirsky, & Lloyd, 2015; Weiss et al., 2016) and deposition of new matrix requiring up-regulation of TGF-β1, VEGF, laminin β1, laminin α2, integrin β1, and dystroglycan receptor (Cattin et al., 2015; Cerriet al., 2014).

Overall, nerve regeneration requires activation of multiple path- ways (Cerri et al., 2014; Chandran et al., 2016) including reorganization of the axonal cytoskeleton, transport of materials, local translation of mRNAs, and the insertion of new membrane and cell surface molecules. In this work, we employed a high sensibility label-free liquid chromatography-mass spectrometry (LC-MS/MS) approach, to analyze and quantify proteins isolated from transected rat sciatic nerves at 20 days after injury directly digested in situ on the tissue slices. This innovative approach allowed the identification of 201 differentially expressed proteins. In addition, gene ontology analysis of proteomic data was conducted in order to categorize differentially expressed proteins by canonical pathways and molecular functions, and to identify possible upstream regulators of our protein dataset. Taken together, our findings showed significant alterations in the expression of proteins associated with cytoskeletal organization and cellular metabolism which further confirm the fine regulation of peripheral nerve regeneration.

2 | MATERIALS AND METHODS

2.1 | Animals and ethics statement

Adult female Sprague–Dawley rats were purchased from Harlan Italy srl, Correzzano, Italy (200–250 gr body mass) and were housed in standard environmental conditions (22 ± 1 °C, 50 ± 5% humidity) with food and water at libitum. Animal care and experimental procedures were performed according to the current Italian and EU animal welfarelegislation (Italian Ministry of Health, authorization n° 109/2014-B).

2.2 | Surgical procedures

Animals were deeply anesthetized using 5% isoflurane and maintained using 2% isoflurane. Nerve injury was carried out by a complete transection of the sciatic nerve. Briefly, rats were fixed in prone position on the operating table. The sciatic nerve was exposed through a longitudinal skin and muscle incision and then cut at the sciatic notch. The proximal and distal nerve ends were immediately reconnected with two sutures at the epineurium using 10–0 silk sutures (end-to-end repair). Thereafter, the nerve was replaced under the muscle and the incision sutured using 3–0 nylon sutures.

2.3 | Tissue processing and histology

To determine the proteomic profile of regenerating sciatic nerve after peripheral nerve transection and end-to-end repair, we performed proteomic analysis at 20 days after injury. Animals were deeply anesthetized with 5% isoflurane and killed by cervical dislocation. Sciatic nerves were removed and fixed in 10% neutral formalin for 24 hr, and conventionally dehydrated, cleared, and embedded in paraffin. Transverse sections, 10 μm in thickness, were collected and aset of equidistantly spaced sections was stained with haematoxylin-eosin to select the injured site.

2.4 | Sample preparation and mass spectrometryanalysis

Formalin-Fixed Paraffin-Embedded (FFPE) blocks were sliced into 10 μm sections. To obtain proteins for LC-MS/MS analysis, formalin was removed and slices were trypsin-digested at room temperature for 2 hr. After digestion procedure, peptides were isolated with three different steps of extraction: 1st step of extraction with trifluoroacetic acid (TFA) 0.1%, 2nd step with 80% Methanol/TFA 0.1%, 3rd step of extraction with 70% Acetonitrile (ACN)/TFA 0.1%. Peptides were then analyzed by MALDI-TOF in positive mode (Ultraflex Extreme, Bruker Daltonics) to assess for protein digestion. Finally, the peptide mixture was acidified by TFA, desalted-concentrated on C-18 ZipTip (Millipore, Burlington, MA), dried under vacuum and then resuspended in 20 μL ofACN/H2O (TFA 0.1%) (2:98, v/v).

Samples were analyzed using an EASY-nLC 1,000 ultra-high- pressure system (Thermo Fisher Scientific, Waltham, MA) coupled via a nano-electrospray ion source (Thermo Fisher Scientific) to a Q- Exactive Orbitrap (Thermo Fisher Scientific), as described (Vergara et al., 2017). In detail, peptides were separated using a 75 μm × 2 cm pre-column with nanoViper fittings (Acclaim pepMap 100, C18, 2 μm, Thermo Fisher Scientific) and a 50 μm ID × 150 mm analytical column with nanoViper fittings (Acclaim PepMap RSLC, C18, 2 μm, Thermo Fisher Scientific). Peptides were eluted with a 2 hr gradientof 5–30% ACN at a flow rate of 300 nL/min.

2.5 | Data analysis

MS raw files were processed using the MaxQuant proteomics software (version 1.5.3.8) (Cox & Mann, 2008, Duhamel et al., 2015), and peptides searched against the *Rattus Norvegicus* UniProt protein database using the Andromeda algorithm (Cox et al., 2011). Trypsin was used as enzyme and two missed cleavages were allowed. Cysteine carbamidomethylation was selected as a fixed modification, N-terminal acetylation, and methionine oxidation as variable modifications. For the MS spectra, an initial mass accuracy of 6 ppm was selected, and the MS/MS tolerance was set to 20 ppm for the HCD data. False discovery rate was set to 1% for peptides and proteins identification. Relative, label-free quantifi- cation of the proteins was conducted using the MaxLFQ algorithm (Cox et al., 2014).

The modulated proteins were uploaded to the web-based Ingenuity Pathway Analysis system (IPA, Qiagen, Hilden, Germany) for functional annotation of proteins, as well as canonical pathway analysis, network discovery, data set correlated disease and function analysis, and upstream analysis. IPA highlights protein networks starting from a continuous updated database of known protein– protein interactions based on direct (physical) and indirect (functional) associations. The algorithm yields a probability score for each possible network. Scores of 10 or higher (negative log of the *p*-value) have a high confidence of not being generated by random chance alone. We also used IPA to identify functionally related genes that correspond to specific canonical pathways that were most significant (−log *p*-value > 5.0) to the data set. To achieve reliable results, we considered only molecules and/or relationships in the rat species and a confidence setting as high predicted or experimental observed (excluding moderate predicted).

IPA provides, also, the principal disease and function categories resulting from some of the modulated proteins of uploaded dataset. Upstream regulator analysis by IPA is based on prior knowledge of expected effects between transcriptional regulators and their target genes from published literature citations stored in the IPA program. This analysis identifies known targets or regulators within the input dataset, if the observed direction of change is mostly consistent with either activation or inhibition of the transcriptional regulator, IPA system performs a prediction and generates a *z* score (*z* scores > 2.0 indicate that a molecule is activated, whereas, *z* scores < −2.0 indicatethe inhibition of target molecules).

2.6 | Immunofluorescence and immunohistochemicalanalysis

Dewaxed sections were rehydrated and washed in 0.1 M PBS and then blocked in 5% goat serum for 1 hr at room temperature. For double immunofluorescence, the slides were incubated overnight at 4 °C with primary rabbit antibodies against DGAT1 (1:100; Santa-Cruz Biotechnol- ogy, Heidelberg, Germany), DGAT2 (1:100; Santa-Cruz Biotechnology) or primary chicken antibody against NF (1:200; Covance, Inc., Princeton, NJ) and with primary mouse antibody against MBP (1:500; Covance, Inc.). After repeated washes with PBS, sections were incubated with Alexa 488-, 594- or 633-conjugated secondary antibodies (1:1000; Invitrogen, Thermo Fisher Scientific) for 2 hr at room temperature and counterstained with nuclear dye 4′-6-Diamidino-2-phenylindole (DAPI, Molecular Probes, Thermo Fisher Scientific). Negative control sections were treated in the same way as described above except that primary antibodies were omitted.

For immunohistochemical staining, sections were incubated with 1% hydrogen peroxide in methanol for 30 min to quench endogenous peroxidase activity and epitopes were retrieved in citrate buffer. Rabbit anti-CD11b (1:100; Abcam, Cambridge, UK), mouse anti-CD68 (1:100; Abcam), rabbit anti-CD45, (1:100; Abcam) and rabbit anti-CD3 (1:100; Abcam) were added to each section and incubated overnight at 4 °C. Thereafter, sections were washed and incubated with the appropriate biotinylated secondary antibody (swine anti-rabbit, 1:200, Dako, Agilent Technologies, Santa Clara, CA, and goat anti-mouse, 1:200, Dako). After washing with PBS, color reaction to peroxidase was performed in 3,3′- diaminobenzidine solution for immunohistochemical staining. Negative control sections were treated in the same way as described above exceptthat primary antibodies were omitted.

3 | RESULTS AND DISCUSSION

3.1 | Proteomic analysis of formalin-fixed paraffin-embedded sections of rat sciatic nerves

In this study, we investigated the proteome of sciatic nerve under regenerating conditions after severe injury (nerve transection and end- to-end repair). Proteome analysis was performed on sciatic nerves at 20 days after injury. This time point has been selected on the basis of the biological events known to occur during nerve repair process such as axonal growth and remyelination (Chen, Yu, & Strickland, 2007). To obtain a proteomic profile specifically associate to the axon growth/ remyelination site, LC-MS/MS analysis was carried out on 10 μm FFPE sections. Histological sections of rat sciatic nerves from control and injured groups were examined to assess morphology and regenerative processes occurring in the different nerves subjected to the proteomic analysis (Figure 1). Nerve sections from control group rats showed evenly distributed nerve axons within the myelin sheath, with no signs of degeneration, inflammatory infiltration, or other abnormalities (Figure 1a–c, uninjured panels). In injured nerves, H&E staining and immunofluorescence analyses showed Schwann cells (SCs) with reactive nuclei, characteristic of synthesis activity, and regenerating axons interacting with SCs (Figure 1a–b, injured panels). Moreover,

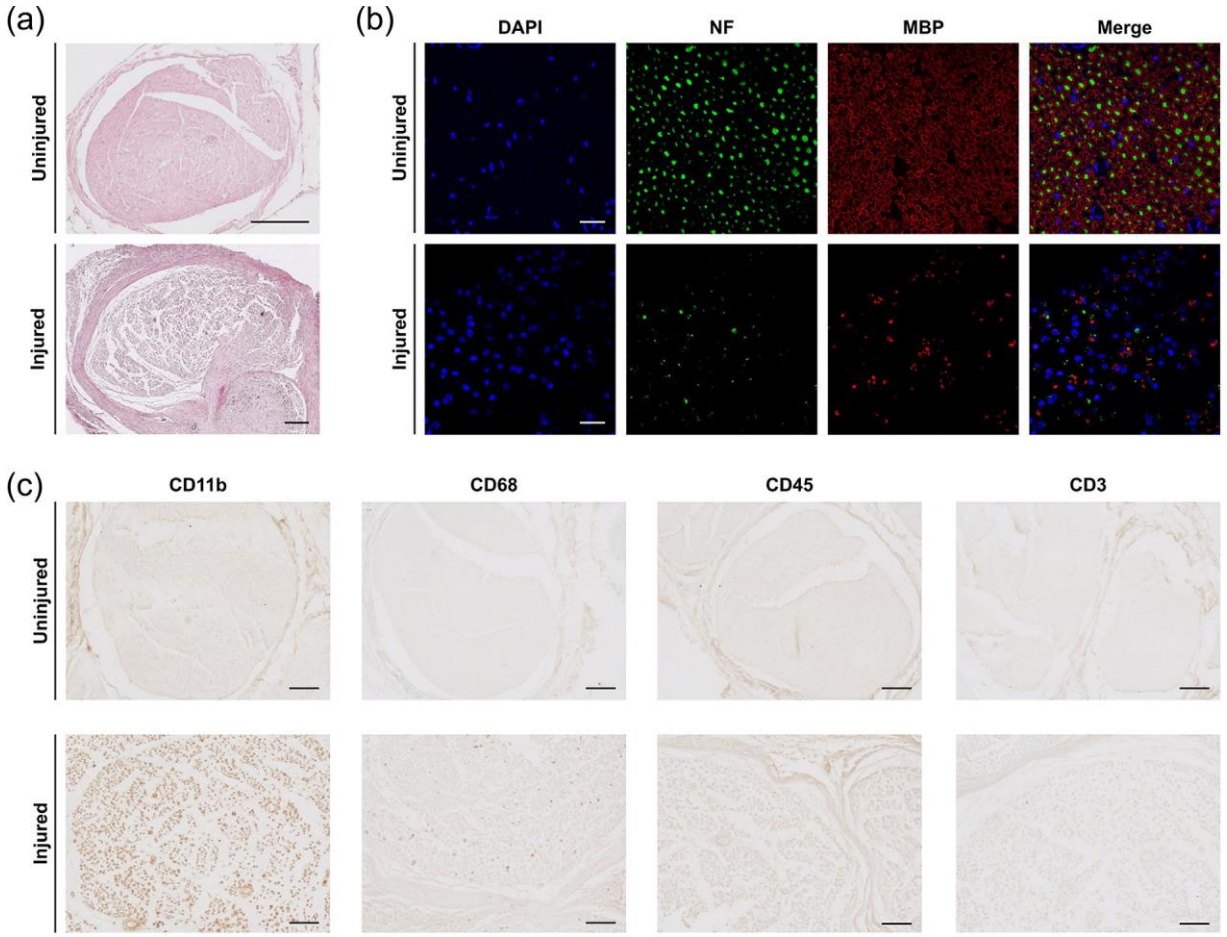

FIGURE 1 (a) Hematoxylin and eosin (H&E) staining of cross-sections of uninjured (intact nerve) or injured (end-to-end repair nerve) rat sciatic nerves at 20 days after transection. Scale bars represent 200 μm. (b) Immunofluorescence staining for axonal marker (neurofilament-M, NF, green) and Schwann cell marker (myelin basic protein, MBP, red) of transverse sections of uninjured/injured rat sciatic nerves at 20 days after transection. Nuclei were counterstained with 4′,6-diamidino-2 phenylindole (DAPI, blue). Scale bars represent 20 μm. (c) Immunohistochemical analysis of immune and inflammatory cell infiltration in uninjured/injured rat sciatic nerves at 20 days after transection. Nerve sections were stained for monocytes/granulocytes marker (CD11b), macrophages marker (CD68), leukocytes marker (CD45), and T cells marker (CD3). Scale bars represent 200 μm

immunohistochemical analysis for monocyte/macrophage markers (CD11b, CD68), leukocyte marker (CD45), and T cell marker (CD3) showed markedly infiltrations of both monocyte and macrophages in the injured nerves (Figure 1c, uninjured vs. injured panels). This confirms other studies that described the presence of multiple cell types at the injured site, creating a cellular microenvironment that can improve the regenerative process (Yi et al., 2015).

FFPE sections of rat sciatic nerves sampled from uninjured (n = 3) and injured (n = 4) groups were analyzed as described in Figure 2a, and subjected to LC-MS/MS analysis and label-free quantification. The resulting identified proteins were subjected to Perseus analysis for the statistical comparison of protein expression profiles. As illustrated by the separation of groups in the two distinct clusters (Figure 2b), nerve regeneration modified significantly the proteomic landscape of peripheral nerve. In detail, proteomic analysis identified 201 differentially expressed proteins that were quantified in at least two of three measurements per group, 62 of them were up-regulated (Table 1) whereas, 139 proteins were down-regulated (Table 2) in the uninjured group with respect to the injured group. Cluster 1 contains proteins down-regulated after injury, and cluster 2 proteins with an increased expression level in injured tissuescompared to uninjured samples (Figure 2b).

3.2 | Canonical pathway and disease and functionanalysis of differentially expressed proteins

To obtain insight into global changes occurring in injured nerve tissues, we then performed a bioinformatics analysis on protein clusters validated after statistical analysis. The biological roles of proteins that were differentially expressed between groups were examined by Ingenuity. At 20 days post nerve injury, four significantly enriched canonical pathways were identified: EIF2 signaling, LXR/RXR activa- tion, acute phase response signaling, and actin cytoskeleton signaling (Supplementary Figure S1). This analysis provided a pathway-based classification view of nerve regeneration with an immediate

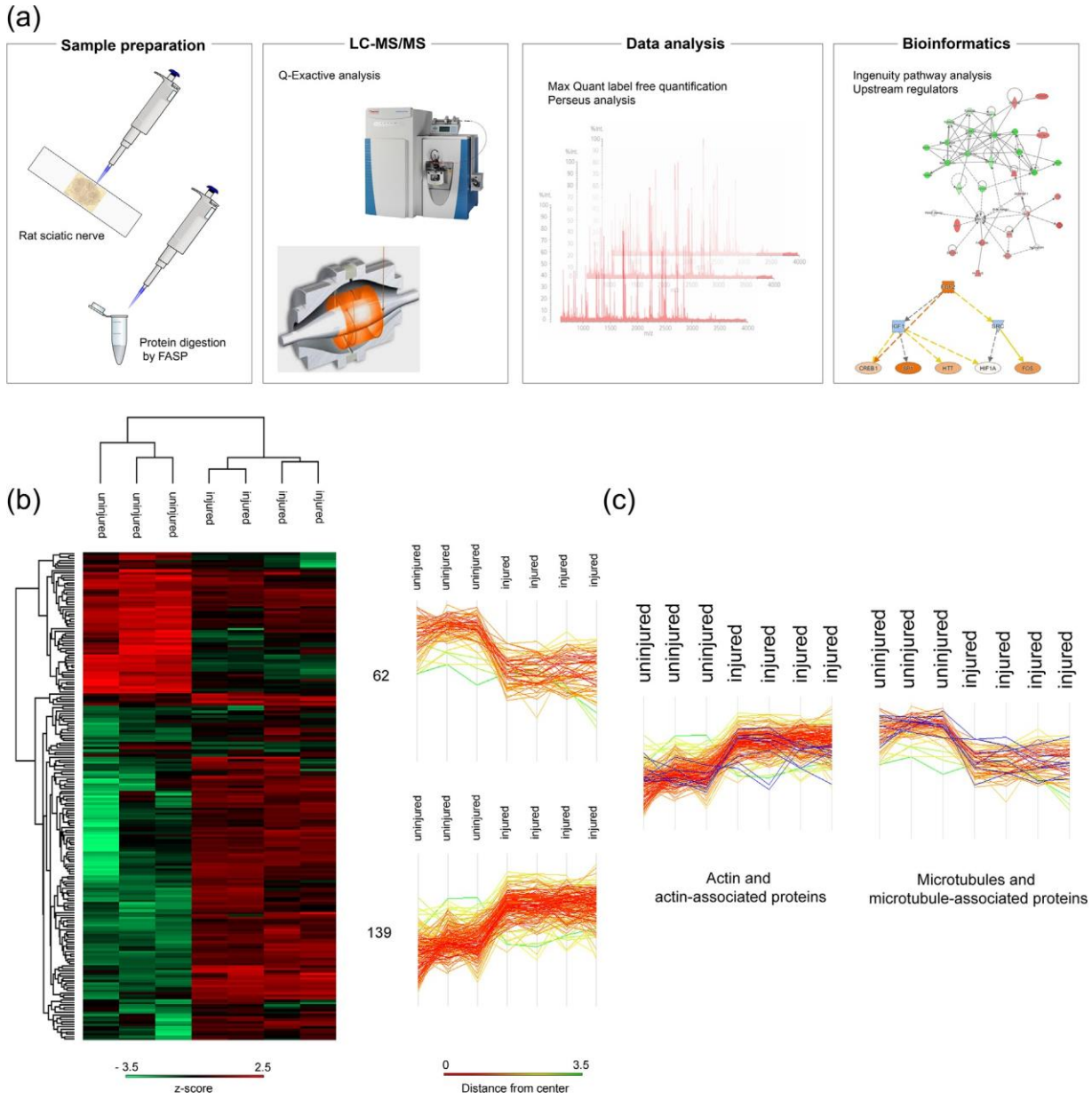

FIGURE 2 LC-MS/MS analysis of peripheral nerve injury. (a) Representative image of the experimental workflow. Proteins were digested in situ, extracted by organic solvents and analysed by MALDI-TOF. Peptides were then desalted and concentrated by ZipTip and analysed by LC-MS/MS. Differentially expressed proteins were subjected to bioinformatics analysis. (b) Hierarchical clustering of genes among wild type and graft samples. Heat map illustrating differential expression of 201 proteins in wild type (n = 3) respect to graft samples (n = 4). Color scale ranges from red to green (highest to lowest relative expression). Two main clusters extracted from A. The windows contain the expression profiles of proteins within clusters. The number of differentially expressed proteins in each cluster is also depicted. (c) The windows contain the expression profiles of proteins within the two main clusters of differentially expressed proteins. Actin and actin-associated proteins, Microtubules and microtubule-associated proteins expression levels are highlighted in blue

interpretation of involved biological processes. Interestingly, two of the enriched pathways, LXR/RXR, and acute phase response signaling, are involved in the regulation of immune responses. These findings are in agreement with the immunohistochemical staining of FFPE nerves tissues, that revealed the presence of immune cells at the injured site, and further extend at proteomic level previous observations that identified by gene expression analysis both pathways as significantlyup-regulated after nerve crush injury (Yi et al., 2015). At the level of

protein synthesis, we found a highly significant enrichment of EIF2 signaling, suggesting an elevated rate of protein synthesis. This demand for protein production at the injury site is in part expected, as demonstrated by the specific spatial localization of the protein synthesis machinery in regenerating axons (Gumy, Tan, & Fawcett, 2010). Moreover, this also highlights that general mechanisms of protein synthesis and degradation may have a major impact on regulating the proteome under regenerating conditions together with

TABLE 1 List of protein down-regulated in injured samples with respect to uninjured group identified by LC-MS/MS analysis

Uniprot IDs	Protein names	Gene names	Peptides	Sequence coverage (%)
P16086	Spectrin alpha chain, non-erythrocytic 1	Sptan1	79	36.2
G3V9M6	Fibrillin 1	Fbn1	5	1.4
Q9R063	Peroxiredoxin-5, mitochondrial	Prdx5	13	54.3
P62986	Ubiquitin-60S ribosomal protein L40	Uba52	13	56.2
P55053	Fatty acid-binding protein, epidermal	Fabp5	7	31.1
O08590	Membrane primary amine oxidase	Aoc3	10	7.9
P12785	Fatty acid synthase	Fasn	17	9.1
P04764	Alpha-enolase	Eno1	32	72.6
P14141	Carbonic anhydrase 3	Ca3	10	47.7
P11232	Thioredoxin	Txn	4	31.4
P15205	Microtubule-associated protein 1B	Map1b	31	16.3
Q3KRE8	Tubulin beta-2B chain	Tubb2b	29	56.4
P85125	Polymerase I and transcript release factor	Ptrf	14	38.8
P15800	Laminin subunit beta-2	Lamb2	35	22.1
P10719	ATP synthase subunit beta	Atp5b	17	38.8
P08010	Glutathione S-transferase Mu 2	Gstm2	8	40.4
P13233	2,3-cyclic-nucleotide 3-phosphodiesterase	Cnp	13	31.4
P48500	Triosephosphate isomerase	Tpi1	11	51
Q01129	Decorin	Dcn	17	36.4
Q6AYC4	Macrophage-capping protein	Capg	15	54.7
Q6P9T8	Tubulin beta-4B chain	Tubb4b	26	55.3
D3ZQN7	Protein Lamb1	Lamb1	21	11.7
P47942	Dihydropyrimidinase-related protein 2	Dpysl2	29	57.3
B5DFC9	Nidogen-2	Nid2	16	15.3
P07943	Aldose reductase	Akr1b1	11	32.6
Q9EQP5	Prolargin	Prelp	23	48.5
P08460	Nidogen-1	Nid1	25	23.8
F1MAA7	Protein Lamc1	Lamc1	30	20.4
Q07936	Annexin A2	Anxa2	34	60.8
P04636	Malate dehydrogenase, mitochondrial	Mdh2	12	44.1
F1LPD0	Protein Col15a1	Col15a1	10	10.8
F1M614	Protein Lama2	Lama2	33	15.5
P42123	L-lactate dehydrogenase B chain	Ldhb	13	35
D3ZVB7	Osteoglycin	Ogn	13	38.9
P04797	Glyceraldehyde-3-phosphate dehydrogenase	Gapdh	30	64.3
P06685	Sodium/potassium-transporting ATPase subunit alpha-1	Atp1a1	20	23.8
Q9Z2S9	Flotillin-2	Flot2	2	6.6
Q6JE36	Protein NDRG1	Ndrg1	8	35.5
P02688	Myelin basic protein	Mbp	23	64.6
P20760	Ig gamma-2A chain C region	Igg-2a	11	35.7
P42930	Heat shock protein beta-1	Hspb1	11	75.7
Q1WIM1	Cell adhesion molecule 4	Cadm4	4	13.4
B4F7C2	Tubulin beta chain	Tubb4a	22	50.5
Q00981	Ubiquitin carboxyl-terminal hydrolase isozyme L1	Uchl1	8	47.5

(Continues)

TABLE 1 (Continued)

Uniprot IDs	Protein names	Gene names	Peptides	Sequence coverage (%)
Q64632	Integrin beta-4	Itgb4	12	8.6
D3ZC55	Heat shock 70 kDa protein 12A	Hspa12a	11	19.1
P06907	Myelin protein P0	Mpz	14	31.5
P04631	Protein S100-B	S100b	2	40.2
P40241	CD9 antigen	Cd9	3	7.5
Q63560	Microtubule-associated protein 6	Map6	10	17.5
P23928	Alpha-crystallin B chain	Cryab	11	69.1
O08557	N(G),N(G)-dimethylarginine dimethylaminohydrolase 1	Ddah1	8	28.8
Q63544	Gamma-synuclein	Sncg	7	56.9
Q4QRB4	Tubulin beta-3 chain	Tubb3	27	58.9
Q6AY56	Tubulin alpha-8 chain	Tuba8	20	41.3
Q9JMB3	Erythrocyte protein band 4.1-like 3	Epb41l3	18	24.7
P07722	Myelin-associated glycoprotein	Mag	7	14.3
P21807	Peripherin	Prph	40	78.6
Q63425	Periaxin	Prx	105	66.3
P16884	Neurofilament heavy polypeptide	Nefh	48	37.6
P12839	Neurofilament medium polypeptide	Nefm	77	65.8
P19527	Neurofilament light polypeptide	Nefl	61	81.5

the regulation at transcriptional level that is generally described in different works (Bosse, Hasenpusch-Theil, Küry, & Müller, 2006; Chandran et al., 2016; Yi et al., 2015). In this scenario, the proteomic approach provided a functional insight into this biological aspect ofnerve regeneration.

In addition to canonical pathways, proteins were also categorized to diseases and functions. Table 3 shows the top over-represented disease and function categories resulting from IPA analysis of differentially expressed proteins. This analysis generated 11 networks with a score ranging from 58 to 9. As shown, Cellular Assembly and Organization, Cell Morphology, Cellular Movement is classified as the top over-represented disease category.

Overall, this suggests that at 20 days after injury, PNS regenera- tion occurs through the coordinated activation of different pathways and networks, which include among the others cytoskeletal and metabolic modifications associated with the expression of proteins and enzymes able to drive cellular growth and to sustain a specific metabolic demand. Spatio-temporal regulation of actin dynamics is essential to sustain axon growth signal (Snider, Zhou, Zhong, & Markus, 2002). As shown in Supplementary Figure S1, Ezrin and Moesin emerged as important regulators of the signaling that acts through the cytoskeleton. These two proteins are components of SCs microvilli, and mediators of diverse cytoskeletal processes, such as cell adhesion and migration, as well as cell morphology. Both proteins are up- regulated after nerve injury, this can be functionally linked to the cellular plasticity required to support nerve regeneration. Actin filaments and microtubules are two major cytoskeletal elements that support nerve assembly after injury. The spatio-temporal regulation of their expressions is pivotal to promote axon regeneration, as these proteins play an instructive role in the regulation of axon growth (Hur & Saijilafu, 2012). As shown in Figure 2c, a different expression of Actin and Actin-associated proteins (Myosin-9, Actin, alpha skeletal muscle, Actin-related protein 2, Actin-related protein 3, F-actin-capping protein subunit alpha-2, Alpha-actinin-1, Alpha-actinin-4), and of microtubules and microtubule-associated proteins (Tubulin beta-4A chain, Microtubule-associated protein 1B, Tubulin beta-4B chain, Tubulin beta-2B chain, Tubulin beta-3 chain, Tubulin beta-8 chain Microtubule-associated protein 6) was observed in our dataset. In detail, Actin and Actin-associated proteins are up-regulated in injured tissues, on the contrary, microtubules and microtubule-associated proteins were down-regulated. Our MS/MS results also showed that Neurofilaments (Neurofilament heavy polypeptide, Neurofilament medium polypeptide, and Neurofilament light polypeptide; Table 2) were down-regulated after nerve injury. This clearly links the MS/MS analysis with the histological characteristics of our samples including the presence of SCs and the absence of neurons in injured tissues, and further again confirms that in situ digestion of tissues allowed definingwith great specificity the sciatic nerve-proteome modifications.

3.3 | A specific metabolic demand support nerverepair

Following an injury, many cell functions are altered. Transcription and translation machineries appear to be activated in the soma (Twiss et al., 2016) and neurotransmitter synthesis decreased (Deumens et al., 2010). A metabolic reprogramming is necessary to sustain the production of proteins and lipids needed for axonal regrowth duringthe regeneration phase. The time course of this biochemical scenario

TABLE 2 List of protein up-regulated in injured samples with respect to uninjured group identified by LC-MS/MS analysis

Uniprot IDs	Protein names	Gene names	Peptides	Sequence coverage (%)
Q9EPH1	Alpha-1B-glycoprotein	A1bg	11	20.1
Q63416	Inter-alpha-trypsin inhibitor heavy chain H3	Itih3	11	23.6
P02651	Apolipoprotein A-IV	Apoa4	10	29.9
P04639	Apolipoprotein A-I	Apoa1	15	48.6
P14046	Alpha-1-inhibitor 3	A1i3	28	23.8
P02650	Apolipoprotein E	Apoe	30	62.5
F1LYQ4		RGD1564515	4	10.1
P62425	60S ribosomal protein L7a	Rpl7a	12	33.6
P07150	Annexin A1	Anxa1	25	56.1
P23593	Apolipoprotein D	Apod	6	30.7
P13635	Ceruloplasmin	Cp	31	29.3
Q6MG61	Chloride intracellular channel protein 1	Clic1	5	30.7
C0JPT7	Filamin alpha	Flna	69	36.2
Q9EPH8	Polyadenylate-binding protein 1	Pabpc1	18	29.4
P07936	Neuromodulin	Gap43	5	32.3
P62907	60S ribosomal protein L10a	Rpl10a	8	27.6
P62853	40S ribosomal protein S25	Rps25	6	34.4
P62630	Elongation factor 1-alpha	Eef1a1	20	32.9
Q63081	Protein disulfide-isomerase A6	Pdia6	16	40.5
Q498U4	SAP domain-containing ribonucleoprotein	Sarnp	6	31.9
Q62812	Myosin-9	Myh9	102	47.1
P70560	Collagen alpha-1(XII) chain	Col12a1	31	23.1
P49744	Thrombospondin-4	Thbs4	3	3.8
P41542	General vesicular transport factor p115	Uso1	7	7.9
D3ZN21	Protein Ddx3y	Ddx3y	9	17.1
Q02874	Core histone macro-H2A.1	H2afy	10	38
P38983	40S ribosomal protein SA	Rpsa	12	40.7
P48679	Prelamin-A/C	Lmna	46	56.8
Q6IMY8	Heterogeneous nuclear ribonucleoprotein U	Hnrnpu	21	21.9
D3ZHA0	Filamin-C	Flnc	35	16.3
P06761	78 kDa glucose-regulated protein	Hspa5	34	53.1
D4AB03	Protein Fam120a	Fam120a	8	10.9
Q9QXQ0	Alpha-actinin-4	Actn4	34	44.6
Q99MZ8	LIM and SH3 domain protein 1	Lasp1	10	33.8
P17074	40S ribosomal protein S19	Rps19	10	49
D3ZH41	Cytoskeleton-associated protein 4	Ckap4	13	47.9
P24368	Peptidyl-prolyl cis-trans isomerase B	Ppib	9	41.2
Q5RKI0	WD repeat-containing protein 1	Wdr1	11	23.3
P11598	Protein disulfide-isomerase A3	Pdia3	33	55.8
Q9QX79	Fetuin-B	Fetub	7	13.7
P29457	Serpin H1	Serpinh1	18	52.8
P04785	Protein disulfide-isomerase	P4hb	26	53.2
Q9Z1A6	Vigilin	Hdlbp	17	15
P31000	Vimentin	Vim	78	93.3

(Continues)

TABLE 2 (Continued)

Uniprot IDs	Protein names	Gene names	Peptides	Sequence coverage (%)
P04256	Heterogeneous nuclear ribonucleoprotein A1	Hnrnpa1	14	43.8
P12346	Serotransferrin	Tf	26	22.6
Q5XFX0	Transgelin-2	Tagln2	14	59.3
P04937	Fibronectin	Fn1	61	32.3
B2RYM3	Inter-alpha trypsin inhibitor, heavy chain 1	Itih1	8	12.8
Q0ZFS8	Protein Srsf3	Srsf3	7	37.8
P21533	60S ribosomal protein L6	Rpl6	15	41.9
Q6PDU1	Serine/arginine-rich splicing factor 2	Srsf2	4	21.7
P18418	Calreticulin	Calr	12	42.1
A7VJC2	Heterogeneous nuclear ribonucleoproteins A2/B1	Hnrnpa2b1	23	61.4
P35053	Glypican-1	Gpc1	4	11.3
P63159	High mobility group protein B1	Hmgb1	7	31
P84100	60S ribosomal protein L19	Rpl19	7	30.6
O35763	Moesin	Msn	34	43.2
Q5EBC0	Inter alpha-trypsin inhibitor, heavy chain 4	Itih4	21	26.2
Q99PF5	Far upstream element-binding protein 2	Khsrp	9	16.1
P01026	Complement C3	C3	44	27.7
P61314	60S ribosomal protein L15	Rpl15	6	28.4
P49242	40S ribosomal protein S3a	Rps3a	10	42.4
Q62733	Lamina-associated polypeptide 2, isoform beta	Tmpo	7	25.7
D3Z9E1	Elastin microfibril interfacer 1	Emilin1	18	27.4
P24268	Cathepsin D	Ctsd	7	18.4
Q6URK4-2	Heterogeneous nuclear ribonucleoprotein A3	Hnrnpa3	19	36.4
Q66HD0	Endoplasmin	Hsp90b1	29	39.3
P62828	GTP-binding nuclear protein Ran	Ran	6	33.3
P10760	Adenosylhomocysteinase	Ahcy	11	29.4
Q6AYI1	DEAD (Asp-Glu-Ala-Asp) box polypeptide 5	Ddx5	17	26.2
P01048	T-kininogen 1	Map1	9	19.3
Q63413	Spliceosome RNA helicase Ddx39b	Ddx39b	12	26.2
G3V6P6	RNA binding motif protein 3	Rbm3	5	34.6
Q62826	Heterogeneous nuclear ribonucleoprotein M	Hnrnpm	25	42.3
G3V852	Protein Tln1	Tln1	53	31
F1LM05	Protein LOC299282	LOC299282	17	30.8
Q63347	26S protease regulatory subunit 7	Psmc2	6	16.6
P04762	Catalase	Cat	8	20.9
P27952	40S ribosomal protein S2	Rps2	9	36.8
Q9JJ54	Heterogeneous nuclear ribonucleoprotein D0	Hnrnpd	5	21.7
P0C0S7	Histone H2A.Z	H2afz	7	36.7
P62914	60S ribosomal protein L11	Rpl11	6	30.9
D3ZAF5	Periostin, osteoblast specific factor	Postn	29	38.9
Q6IRK9	Carboxypeptidase Q	Cpq	8	25
P02793	Ferritin light chain 1	Ftl1	13	67.2
P06399	Fibrinogen alpha chain	Fga	28	44
P24049	60S ribosomal protein L17	Rpl17	8	42.4

(Continues)

TABLE 2 (Continued)

Uniprot IDs	Protein names	Gene names	Peptides	Sequence coverage (%)
Q9QX81	Protein Hnrnpab	Hnrnpab	8	24.9
P70615	Lamin-B1	Lmnb1	21	34.6
M0R9Q1	Protein Rbm14	LOC100911677	12	22
Q5M7U6	Actin-related protein 2	Actr2	6	20.3
G3V7Q7	IQ motif containing GTPase activating protein 1	Iqgap1	34	23.7
P61354	60S ribosomal protein L27	Rpl27	6	43.4
P62804	Histone H4	Hist1h4b	20	66
P02680	Fibrinogen gamma chain	Fgg	13	34.6
P08699	Galectin-3	Lgals3	4	18.7
P13383	Nucleolin	Ncl	14	18.5
D3ZBN0	Histone H1.5	Hist1h1b	13	38.7
P62083	40S ribosomal protein S7	Rps7	11	44.3
P04041	Glutathione peroxidase 1	Gpx1	12	58.7
Q5FVH2	Phospholipase D3	Pld3	5	13.3
P83732	60S ribosomal protein L24	Rpl24	4	19.7
Q62667	Major vault protein	Mvp	26	37.4
Q00438	Polypyrimidine tract-binding protein 1	Ptbp1	11	35.3
P20059	Hemopexin	Hpx	13	22.8
F1LM30	Protein Ighm	ghm	5	11.1
P51635	Alcohol dehydrogenase [NADP(+)]	Akr1a1	13	44.6
P63326	40S ribosomal protein S10	Rps10	4	23.6
P31977	Ezrin	Ezr	13	19.8
P62632	Elongation factor 1-alpha 2	Eef1a2	14	33.3
P70560	Collagen alpha-1(XII) chain	Col12a1	31	23.1
P21263	Nestin	Nes	42	27.9
G3V9R8	Heterogeneous nuclear ribonucleoprotein C	Hnrnpc	8	26.8
P0C170	Histone H2A type 1-E	Hist1H2ae	12	62.9
Q00729	Histone H2B type 1-A	Hist1h2ba	24	83.3
P14480	Fibrinogen beta chain	Fgb	20	43.2
P84245	Histone H3.3	H3f3b	16	41.2
P08932	T-kininogen 2	N/A	10	23.7
P43278	Histone H1.0	H1f0	10	35.6
M0R7B4	Protein LOC684828	LOC684828	23	42.6
P48675	Desmin	Des	26	55.7
P07335	Creatine kinase B-type	Ckb	19	56.7
P23358	60S ribosomal protein L12	Rpl12	4	24.8
D3ZZT9	Protein Col14a1	Col14a1	43	30.3
P68136	Actin, alpha skeletal muscle	Acta1	51	72.9
P11030	Acyl-CoA-binding protein	Dbi	5	48.3
Q4V7C7	Actin-related protein 3	Actr3	13	35.2
Q3T1K5	F-actin-capping protein subunit alpha-2	Capza2	5	26.6
P29826	Rano class II histocompatibility antigen, B-1 beta chain	RT1-Bb	3	8.4
P04642	L-lactate dehydrogenase A chain	Ldha	20	46.7
Q91ZN1	Coronin-1A	Coro1a	13	29.9

(Continues)

TABLE 2 (Continued)

Uniprot IDs	Protein names	Gene names	Peptides	Sequence coverage (%)
F1LZF4	Protein Col6a5	Col6a5	30	13.3
Q80ZA3	Alpha-2 antiplasmin	Serpinf1	10	30.1
Q5XI73	Rho GDP-dissociation inhibitor 1	Arhgdia	9	48.5
G3V8L7	Integrin alpha M	Itgam	10	11.6
O35567	Bifunctional purine biosynthesis protein PURH	Atic	14	35.6
Q9Z1P2	Alpha-actinin-1	Actn1	33	37.8
Q5XI38	Lymphocyte cytosolic protein 1	Lcp1	20	34.6

suggests that at 3 weeks after injury, Apolipoproteins (Apo) levels are increased, de novo cholesterol synthesis remains low, myelin cholesterol is reincorporated into new myelin following Wallerian degeneration, and macrophages are loaded with myelin debris to produce lipid droplets (Goodrum, Earnhardt, Goines, & Bouldin, 1994). In line with this metabolic hypothesis, ApoA4, ApoA1, ApoE, and ApoD resulted significantly overexpressed in injured tissues (Table 2), and were included in the Free Radical Scavenging, Small Molecule Biochemistry, Lipid Metabolism network identified after IPA analysis (Figure 3). Overall, we confirmed that up-regulation of Apo proteins at the injury site, and confirmed the proteomic changes observed by two- dimensional electrophoresis and MS by Jiménez et al. (2005) on injured rat sciatic nerve. At the injury site, ApoD potentiates macrophage- myelin interaction, and is needed for appropriate Galectin-3 expres- sion of naïve macrophages upon exposure to myelin (García-Mateo et al., 2014). Galectin is among the protein up-regulated in our MS/MS dataset (Table 2). Moreover, injury to peripheral nerves is known to activate an inflammatory response in Schwann cells. We identified in this context key damage-associated molecular pattern molecule like the high mobility group box 1 (HMGB1), complement C3 or Immunoglobulin heavy constant mu (IgHm). HMGB1 has recently demonstrated to be implicated in pathway activating the inflammatory response in Schwann cells following peripheral nerve injury (Man et al., 2015), as well as antibody (IgG). IgG2b against myelin glycoproteins, has already been reported in Wallerian degeneration (Kubo, Yamashita, Yamaguchi, Hosokawa, & Tohyama, 2002) and C3 in macrophages. Complement components play a critical role both in macrophage invasion of degenerating nerves and in the ingestion ofmyelin by these cells (Brück & Friede, 1991).

We reasoned that the increased expression of Apo proteins may be associated at cellular level with a higher expression of proteins involved in lipid uptake and fatty acid metabolism. In parallel with the changes observed for Apo proteins, Caveolin, a protein necessary to fatty acid uptake was among the proteins identified in the Free Radical Scavenging, Small Molecule Biochemistry, Lipid Metabolism network (Table 3 and Figure 3). Caveolin has a role in the generation of lipid droplets and was functionally linked to the myelinating phenotype of SCs (Mikol, Scherer, Duckett, Hong, & Feldman, 2002).

A metabolic hypothesis seems to emerge from these data, SCs decreased fatty acid de novo synthesis using free fatty acids and other substrates, products of membrane degradation during Wallerian degeneration, and increased the expression of enzymes involved in triacylglycerol biosynthesis, storage, and lipolysis.

As validation of this hypothesis, we investigated the protein expression of DGAT1 and DGAT2 that catalyze the final step in the biosynthesis of TGs. The expression of DGAT1/2 proteins was assessed by immunofluorescence using adjacent sections of the same sciatic nerves employed for proteomic analysis (Figure 4). A marked increase in DGAT1 (Figure 4a) and DGAT2 (Figure 4b) staining was observed in the injured/regenerating nerves compared with nerve from control group. The induction of DGAT1/2 in peripheral nerves was observed in Schwann cells as revealed by co-staining with the Schwann cell marker MBP (Figure 4). Interestingly, the expression of the metabolic enzymes DGAT1 and DGAT2 in Schwann cells appeared timely regulated when tested in sciatic nerve after crush injury. In particular, the expression of DGAT1/2 increased at day 10 and day 20 after crush injury and decreased towards healthy control nerve at day 40 suggesting that the expression of these enzymes is regulated in injured nerves to allow lipid re-utilization and to support the different phases of axonal/nerve regeneration (see Supplementary Figures S2 and S3). This metabolic program is also confirmed by the down- regulation of fatty acid synthase (FASN), the primary enzyme of lipid denovo synthesis, observed in injured tissues (Table 1).

Nerve injury induces bioenergetics dysfunction characterized by reduced glycolytic capacity (Lim, Rone, Lee, Antel, & Zhang, 2015), and increased oxidative stress (Lanza et al., 2012). In fact, glucose metabolism enzymes, lactate dehydrogenase b (LDHb), Glyceralde- hyde 3-phosphate dehydrogenase (GAPDH), malate dehydrogenase, and ATP synthase subunit beta (ATP5b) were down-regulated (Table 1). Among other pathways displaying significant changes, differences in the expression of proteins involved in the metabolism of reactive oxygen species (ROSs) were observed. Specifically, Glutathi- one peroxidase 1 (GPX1) and Catalase were up-regulated, while Peroxiredoxin-5 (Prdx5) was down-regulated at injured site (Tables 1 and 2, Figure 3) as a result of the increased oxidative stress at injured site (Lanza et al., 2012).

4 | CONCLUSIONS

Here, we applied a proteomic workflow for label-free analysis of injured nerve tissues. To date, proteomic studies on peripheral

TABLE 3 Top disease and function categories as determined by IPA pathways analysis. A list of genes that contribute to each of the significant categories is reported

Top diseases and functions	Score	F.M.	Molecules in network
Cellular assembly and organization, cell morphology, cellular movement	58	31	AHCY, ANXA1, CADM4, calpain, CAPZA2, CD9, COL12A1, Collagen type I, DDX5, FLNA, FLNC, FN1, H2AFY, HNRNPA1, HNRNPM, ITGB4, KHSRP, Kng1/Kng111, Lamin b, LGALS3, LMNA, LMNB1, Mapk, MDH2, Nes, PTBP1, RAN, RPL12, RPL10A, SERPINH1, SRSF2, TAGLN2, TMPO, VIM, WDR1
Cancer, organismal injury and abnormalities, reproductive system disease	44	26	A1BG, a-tub, b-tub, CNP, DDX39B, DPYSL2, EMILIN1, ERK1/2, FAM120A, Ferritin, GPC1, HDL, hemoglobin, Hmgb1, Hnrnpa3, HPX, ITIH4, MAP6, MAP1B, NEFH, NEFL, Nefm, PDGF (family), PI3K (family), PRPH, S100B, SARNP, SERPINF1, TF, TUBA8, TUBB3, TUBB2B, TUBB4A, TUBB4B, tubulin (family)
Cancer, cell death and survival, organismal injury and abnormalities	37	23	20s proteasome, 26s Proteasome, AKR1B1, ANXA2, CAPG, CTSD, Cyclin D, Cyclin E, cytochrome C, Cytokeratin, EEF1A2, HNRNPC, HNRNPD, HNRNPU, Hsp27, Hsp70, NDRG1, PABPC1, PARP, PI3K (complex), PSMC2, Rnr, RPL15, RPL19, RPL24, RPL27, RPS2, RPS7, RPS10, RPS19, RPS25, RPSA, SNCG, Ubiquitin, UCHL1
Developmental disorder, hematological disease, hereditary disorder	33	21	AOC3, C3, C1q, CALR, Collagen type IV, Collagen(s), Complement component 1, elastase, FGA, FGB, FGG, Fibrin, Fibrinogen, HSP90B1, Integrin, Integrin alpha V beta 3, LAMB1, LAMB2, LAMC1, Laminin, Laminin1, Ldha/RGD1562690, NFkB (complex), NID1, NID2, P4HB, Pdgf (complex), PDIA3, PDIA6, PPIB, PRELP, Rap1, RBM3, THBS4, TLN1
Hereditary disorder, organismal injury and abnormalities, skeletal and muscular disorders	33	21	Calmodulin, Ck2, CKB, CRYAB, DDAH1, EEF1A1, ENO1, EPB41L3, ER, GAPDH, H2AFZ, H3F3A/H3F3B, HDLBP, Hist1h1b, HIST1H2BA, HISTONE, Histone h3, Histone h4, HNRNPA2B1, HSP, HSPA5, HSPA12A, HSPB1, IgG2a, LDHB, MPZ, NCL, p85 (pik3r), Pka, RBM14, RNA polymerase II, SRC (family), USO1, Vegf, voltage-gated calcium channel
Cellular assembly and organization, cellular function and maintenance, cell morphology	28	19	Actin, ACTN1, ACTN4, ACTR2, ACTR3, Akt, aldo, Alpha actin, Alpha Actinin, Alpha catenin, ARHGDIA, Arp2/3, CORO1A, CP, DES, EF-1 alpha, Erm, EZR, F Actin, IQGAP1, LAMA2, Laminin2, LCP1, MAG, Mbp, MSN, MYH9, Myosin, P glycoprotein, PRX, Rho gdi, Rock, Spectrin, SPTAN1, SRSF3
Free radical scavenging, small molecule biochemistry, lipid metabolism	24	17	AMPK, APOA1, APOA4, APOD, APOE, CAT, Caveolin, chymotrypsin, CKAP4, CLIC1, Collagen Alpha1, DCN, ERK, FABP5, FBN1, FLOT2, GPX1, HDL-cholesterol, LASP1, Ldh (complex), LDL, LDL-cholesterol, LRP, MVP, NADPH oxidase, Nr1h, PRDX5, PRKAA, Pro-inflammatory Cytokine, PTRF, RPL17, SAA, Sod, trypsin, VLDL-cholesterol
Hair and skin development and function, nephrosis, organismal injury and abnormalities	19	14	ACTA1, ADCY, ADRB, Alp, ATP1A1, ATP5B, CA3, CaMKII, caspase, CD3, Cofilin, COL14A1, Creb, Cyclin A, DBI, FASN, FTL, Gsk3, GSTM1, Hsp90, IL1, Insulin, Lh, MTORC1, OGN, P38 MAPK, Pkc(s), Pkg, Pld, PLD3, PP2A, Ras homolog, RPL6, Tpi1 (includes others), TXN
Behavior, neurological disease, immunological disease	10	9	ADCY3, ADGRG1, ADRA2B, ADRA2C, ADRB2, ALDH6A1, ANGPTL3, APRT, ARL8B, ATIC, Basp1, CKMT1A/CKMT1B, CRAT, D1Pas1, DLG4, ECI1, EHD4, GPRC5B, Hspg, IgG1, INSR, KLHL17, Ldha/RGD1562690, LRRC7, MAPK3, Mug1 (includes others), Nefm, Pak2, PRPH, PTPN5, Rps3a1, SDK1, SNCG, Uba52, UBC
Cancer, cell-to-cell signaling and interaction, cellular development	9	8	Ap1, BCR (complex), FETUB, GAP43, HLA-DQB1, IFN Beta, Ige, IgG, Igm, IL12 (complex), Immunoglobulin, Interferon alpha, ITIH1, ITIH3, JINK1/2, Jnk, MAP2K1/2, Mek, MHC Class I (complex), NFAT (complex), Nfat (family), p70 S6k, PDGF BB, PLC gamma, POSTN, Rar, Ras, RPL11, RPL7A, Rxr, Sos, TCR, Tgf beta, transglutaminase, TSH
Dermatological diseases and conditions, inflammatory disease, organismal injury and abnormalities	9	8	AHR, AKR1A1, AKR1C1/AKR1C2, ASPN, ATP9A, COL11A1, COL12A1, COL6A1, COL6A5, CPQ, EMILIN1, FSH, GOT, GPRC5B, H1f0, HABP2, Hist1h1e, Histone H1, IGF1, Inhibin, ITGAM, LOC299282, LPAR2, LPAR4, LTBP2, Mmp, PDGF-AA, Pdgfr, PLC, PYY, Rac, S1PR3, SLC12A7, SLIT3, TGFB1

FM, focus molecules.

IPA analysis was done on the list of 201 proteins differentially expressed in sciatic nerve from control and graft rat groups.

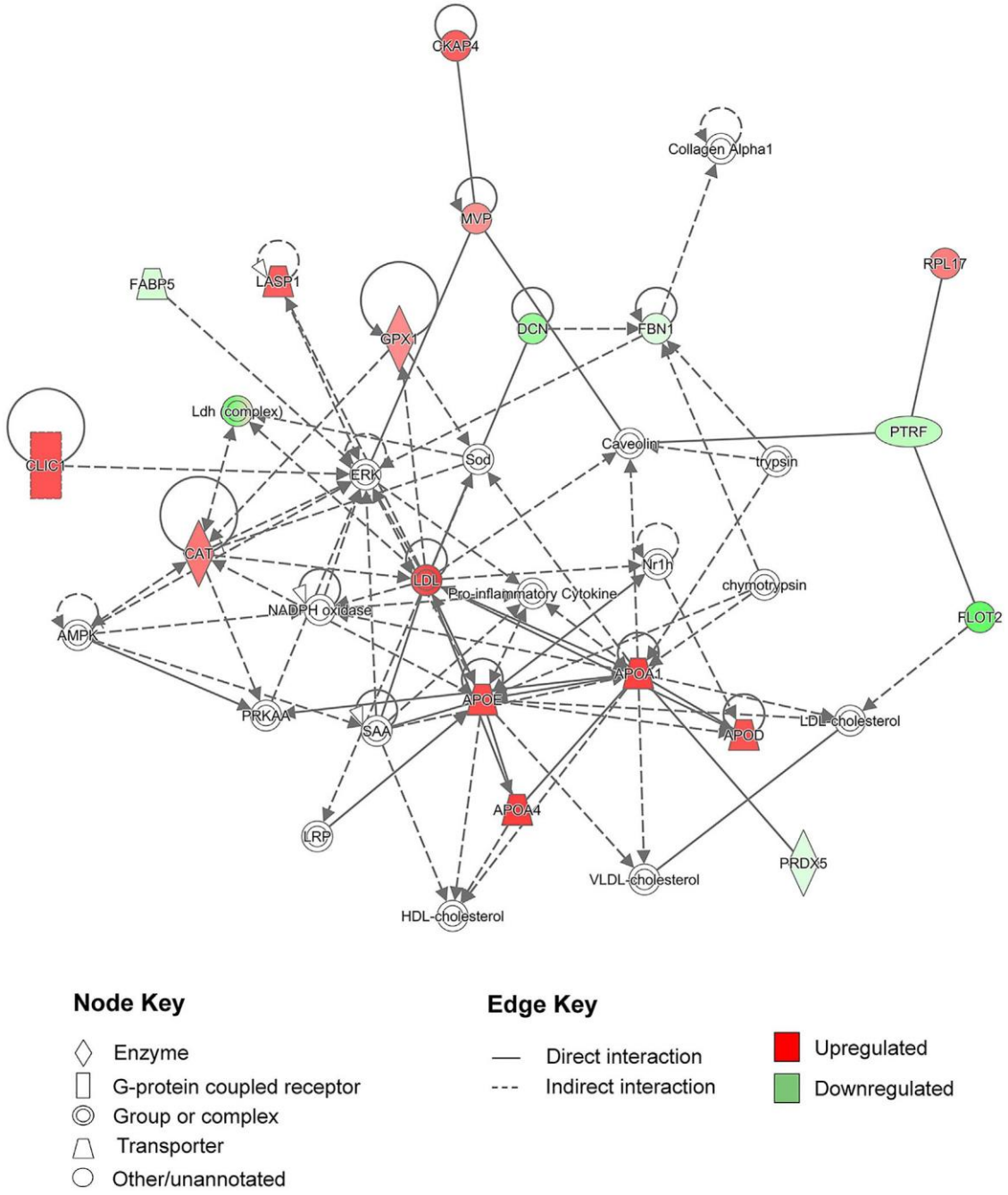

FIGURE 3 Free radical scavenging, small molecule biochemistry, lipid metabolism network. Proteins in the network are displayed as a series of nodes and edges (corresponding to biological relationships between nodes). Nodes are displayed using shapes that represent the functional class of the proteins, as indicated in the key. Red and green color indicates genes significantly increased and decreased in expression, respectively. White nodes indicate no significant change in protein expression. The straight lines represent direct relationships and the dotted lines represent indirect relationships. Symbols used in the figure represent: vertical rhombus, enzyme; horizontal rectangle, G-protein coupled receptor; trapezoid, transporter; circle, other; concentric circles, complex/group

nerve injury/regeneration have analyzed large regions of the tissue rather than to perform site-injury specific proteomics. We carried out localized proteomics on single FFPE nerve sections to determine differentially expressed proteins in rat nerve during the first phase of the axonal growth/remyelination process (20 days after nerve transection injury and end-to-end repair). This approach allowed the identification of hundreds of proteins at nerve specific site-injury. Canonical functions and network analysis showed that processes associated with cytoskeletal remodeling and cellular metabolism are modulated at the injured sites. Modification of proteins associated with cellular metabolism is particularly intriguing because it implies the activation of a specific metabolic program capable to sustain a peculiar metabolic demand. Some actors were identified in this work. In addition to the

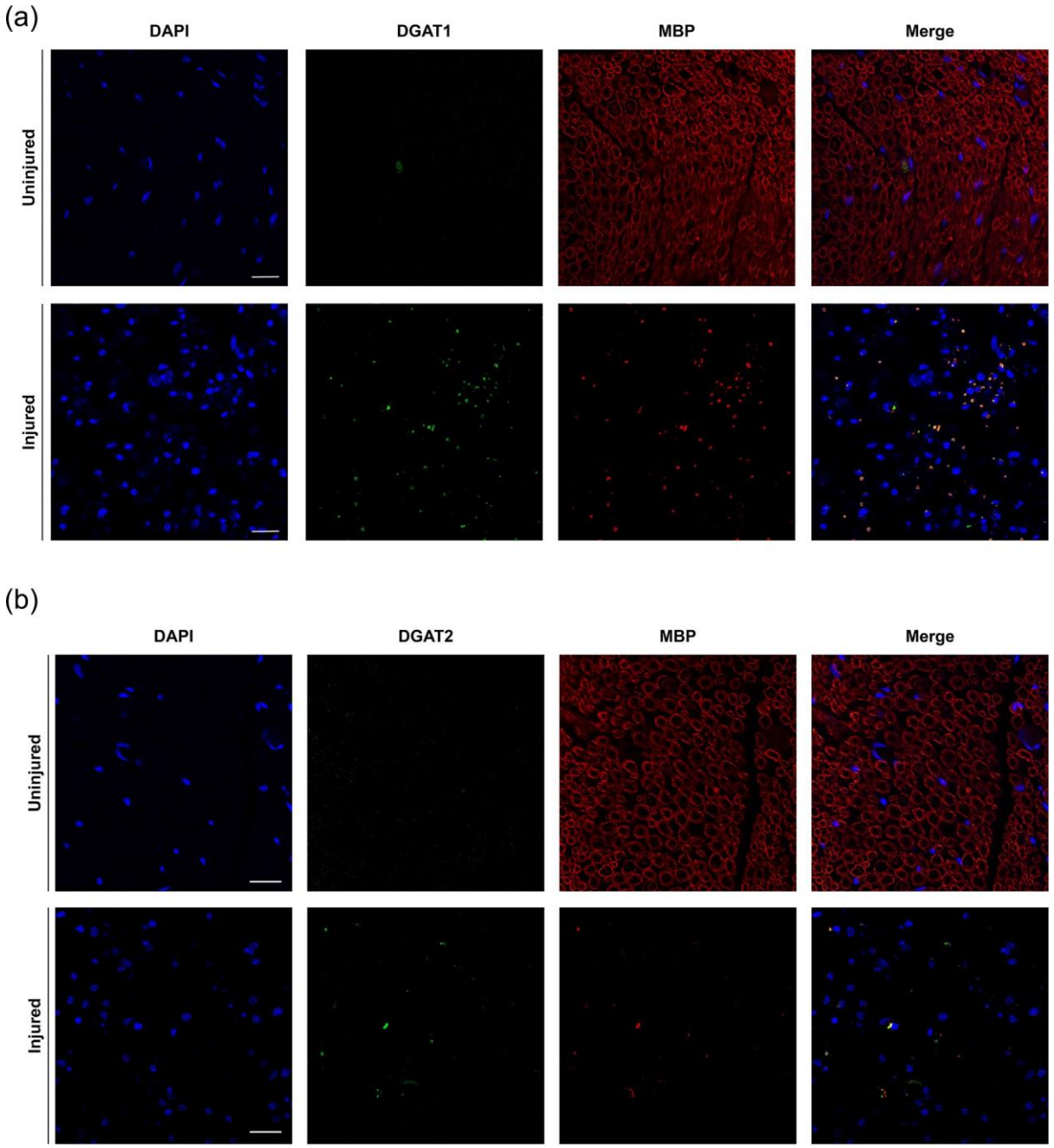

FIGURE 4 Confocal images of cross-sections of uninjured (intact nerve) and injured (end-to-end repair nerve) rat sciatic nerves at 20 days after transaction. (a) Nerve sections stained with antibodies for diacylglycerol O-acyltransferase 1 (DGAT1, green) and myelin basic protein (MBP, red). Nuclei were stained with 4′,6-diamidino-2 phenylindole (DAPI, blue). (b) Nerve sections stained with antibodies for diacylglycerol O-acyltransferase 2 (DGAT2, green) and MBP, red. Nuclei were stained DAPI, blue. Scale bars represent 20 μm

well-known role of Apo proteins, we propose that the higher uptake of lipids from SCs at the injury site provide the supply for the biosynthesis of TGs by DGAT enzymes. Here, we demonstrated for the first time a role for DGAT1 and DGAT2 in the process of nerve regeneration. Metabolic pathways do not work in isolation. Increased expression of DGAT1/2 correlated with the increased expression of Apo proteins and reduced expression of FASN.

The proteomic differences identified by LC-MS/MS may be under the control of a complex set of transcriptional factors and other potential regulators. We used IPA to generate a list of possible upstream regulators, namely factors that may have a role of repression or activation of our dataset. These proteins are listed in Table 4. Among these, specificity protein 1 (SP1), which is involved in nerve regeneration (Kiryu-Seo & Kiyama, 2011), has a role of regulation of metabolic proteins discussed above, including Apo and FASN. This potentially provides a link between proteomic data and transcriptional machinery that drive nerve regeneration.

TABLE 4 Main upstream regulator as determined by ipa pathways analysis

Upstream regulator	Molecule type	Predicte activation dstate	Activation *z*-score	*p*-value of overlap	Target molecules in dataset
KRAS	Enzyme	Activated	3,44	0,0000461	ACTR3, CRYAB, DDAH1, EEF1A1, FBN1, FLOT2, FN1, HSPA5, HSPB1, PDIA3, PRPH, RPSA, Tpi1 (includes others), VIM
IL6	Cytokine	Activated	2,771	0,000677	ANXA1, APOA1, APOE, C3, CP, DCN, FGA, FGB, FGG, FN1, GAP43, HPX, HSPA5, ITGAM, PRPH, TF, VIM
ANGPT2	Growth factor	Activated	2,579	0,000000119	ACTA1, CALR, CAT, CRYAB, FN1, HSPA5, P4HB, PDIA3, PDIA6, POSTN, RBM14, TUBB3, VIM
SMARCA4	Transcription regulator	Activated	2,433	0,000583	ACTA1, ACTN4, APOA1, CNP, CP, DES, FGG, FN1, GAPDH, GPX1, LGALS3, LMNA, MAP1B, SERPINH1, VIM
P38 MAPK	Group	Activated	2,386	0,0292	DES, FLNA, FN1, HSPA5, ITGAM, ITGB4, Nes, POSTN
STAT3	Transcription regulator	Activated	2,243	0,000726	APOA4, CAT, CD9, FASN, FGA, FGB, FGG, FN1, GAP43, HNRNPD, ITGAM,LDHB, NDRG1, VIM
MMP3	Peptidase	Activated	2,236	0,00407	NDRG1, RBM14, SRSF2, SRSF3, VIM
NFE2L2	Transcription regulator	Activated	2,231	0,00000021	AKR1A1, APOA4, ATP1A1, CAT, CTSD, DDX39B, FN1, FTL, GPX1, GSTM1, HSP90B1, LMNA, PDIA3, PDIA6, PPIB, RAN, TXN, USO1
EDN1	Cytokine	Activated	2,226	0,0000468	ACTA1, ANXA1, EZR, FN1, HSPA5, ITGAM, MSN, PDIA6, RPSA, VIM
CSF1	Cytokine	Activated	2,215	0,0334	APOE, FN1, HSP90B1, HSPA5, ITGAM
PRNP	Other	Activated	2,213	0,000104	APOE, CTSD, HSP90B1, HSPA5, HSPB1, PDIA3
LEP	Growth factor	Activated	2,196	0,00243	APOA1, APOA4, CA3, FASN, GAP43, GAPDH, GPX1, HPX, HSPA5, ITGAM, Kng1/Kng1l1, VIM
IFNG	Cytokine	Activated	2,084	0,0017	AHCY, ATP1A1, C3, CAT, CORO1A, CP, CTSD, DDX5, EEF1A1, FABP5, FASN, FGG, FN1, FTL, HLA-DQB1, Hnrnpa3, HSPB1, ITGAM, LAMB2, LAMC1, Ldha/RGD1562690, LGALS3, MYH9, SERPINH1
FGF2	Growth factor	Activated	2,069	0,000000233	AKR1B1,CAPZA2,CNP,CRYAB,DCN, ENO1,FBN1,FLNA,FN1,GAP43,Ldha/ RGD1562690,LMNA,MPZ,Nes,TF, TUBB3,VIM
SP1	Transcription regulator	Activated	2,06	0,000171	APOA1, APOE, ATP5B, CAT, CKB, CRYAB, CTSD, EZR, FASN, FLNA, FN1, HSPA5, ITGAM, NDRG1, SNCG, VIM
EGF	Growth factor	Activated	2	0,002	ACTN1, APOA1, CTSD, DCN, DDX5, EEF1A1, EZR, FASN, FN1, ITGAM,NCL, PPIB, VIM
IPMK	Kinase	Activated	2	0,0000905	CORO1A, FLNA, FLNC, TAGLN2
KIAA1524	Other	Activated	2	0,0041	CRYAB, DCN, LASP1, NCL
PDGF (family)	Group	Activated	2	0,00000175	CALR, P4HB, PDIA3, VIM

TABLE 4

Upstream regulator	Molecule type	Predicte activation dstate	Activation *z*-score	*p*-value of overlap	Target molecules in dataset
TGM2	Enzyme	Activated 2		0,16	ACTA1, C3, FN1, ITGAM
RHO	G-protein coupled receptor	Activated 2		0,0041	HIST1H2BA, LAMB2, NID1, PRPH
NUPR1	Transcriptionregulator	Inhibited	−2,449	0,379	HNRNPA2B1, HNRNPM, LMNB1, NDRG1, RBM14, TMPO
RICTOR	Other	Inhibited	−2,387	2,11E-08	ATP5B, FABP5, Mbp, PSMC2, RPL10A, RPL11, RPL12, RPL17, RPL6, RPL7A, RPS10, RPS19, RPS2, Rps3a1, RPSA, Uba52
Lh	Complex	Inhibited	−2,236	0,0406	ACTA1, ACTN1, ACTR2, EZR, FLNC,TLN1
HSF1	Transcriptionregulator	Inhibited	−2,128	0,0101	CRYAB, FASN, HSPB1, SERPINH1,SPTAN1, TUBB4A
MTOR	Kinase	Inhibited	−2,034	7,91E-12	AKR1A1, AKR1B1, CNP, ENO1, FABP5, FASN, FGB, FN1, GAP43, HSP90B1, HSPB1, LDHB, MAG, MDH2, PPIB, PRDX5, PRX, PTBP1, RPL12, SNCG

ACKNOWLEDGMENTS

The authors acknowledge the National Operational Programme for Research and Competitiveness (PONREC) “RINOVATIS” (PON02_00563_3448479). We gratefully acknowledge funding from the Apulia Regional Cluster project “SISTEMA” project code T7WGSJ3. This research was supported by SIRIC ONCOLille Grant INCa-DGOS-Inserm 6041aa.

ORCID

Daniele Vergara http://orcid.org/0000-0002-2396-7674

REFERENCES

Abe, N., & Cavalli, V. (2008). Nerve injury signaling. *Current Opinion inNeurobiology*, *18*(3), 276–283.

Bosse, F., Hasenpusch-Theil, K., Küry, P., & Müller, H. W. (2006). Gene expression profiling reveals that peripheral nerve regeneration is a consequence of both novel injury-dependent and reactivated develop- mental processes. *Journal of Neurochemistry*, *96*(5), 1441–1457.

Brück, W., & Friede, R. L. (1991). The role of complement in myelin phagocytosis during PNS wallerian degeneration. *Journal of the Neurological Sciences*, *103*(2), 182–187.

Cattin, A. L., Burden, J. J., Van Emmenis, L., Mackenzie, F. E., Hoving, J. J., Garcia Calavia, N., … Lloyd, A. C. (2015). Macrophage-induced blood vessels guide schwann cell-mediated regeneration of peripheral nerves.*Cell*, *162*(5), 1127–1139.

Cerri, F., Salvatore, L., Memon, D., Martinelli Boneschi, F., Madaghiele, M., Brambilla, P., … Quattrini, A. (2014). Peripheral nerve morpho- genesis induced by scaffold micropatterning. *Biomaterials*, *35*(13), 4035–4045.

Chan, K. M., Gordon, T., Zochodne, D. W., & Power, H. A. (2014). Improving peripheral nerve regeneration: From molecular mechanisms to potential therapeutic targets. *Experimental Neurology*, *261*, 826–835.Chandran, V., Coppola, G., Nawabi, H., Omura, T., Versano, R., Huebner, E. A., ... Geschwind, D. H. (2016). A systems-level analysis of the peripheralnerve intrinsic axonal growth program. *Neuron*, *89*(5), 956–970.

Chen, Z. L., Yu, W. M., & Strickland, S. (2007). Peripheral regeneration.
Annual Review of Neuroscience, *30*, 209–233.

Cox, J., & Mann, M. (2008). MaxQuant enables high peptide identification rates, individualized p.p.b.-range mass accuracies and proteome-wide protein quantification. *Nature Biotechnology*, *26*(12), 1367–1372.

Cox, J., Neuhauser, N., Michalski, A., Scheltema, R. A., Olsen, J. V., & Mann,
M. (2011). Andromeda: A peptide search engine integrated into the MaxQuant environment. *Journal of Proteome Research*, *10*(4), 1794–1805.

Cox, J., Hein, M. Y., Luber, C. A., Paron, I., Nagaraj, N., & Mann, M. (2014). Accurate proteome-wide label-free quantification by delayed normali- zation and maximal peptide ratio extraction, termed MaxLFQ. *Molecular& Cellular Proteomics*, *13*(9), 2513–2526.

Deumens, R., Bozkurt, A., Meek, M. F., Marcus, M. A., Joosten, E. A., Weis, J., & Brook, G. A. (2010). Repairing injured peripheral nerves: Bridging the gap. *Progress in Neurobiology*, *92*(3), 245–276.

Duhamel, M., Rodet, F., Delhem, N., Vanden Abeele, F., Kobeissy, F., Nataf, S., … Salzet, M. (2015). Molecular consequences of proprotein convertase 1/3 (PC1/3) inhibition in macrophages for application to cancer immunotherapy: A proteomic study. *Molecular & Cellular Proteomics*, *14*(11), 2857–2877.

García-Mateo, N., Ganfornina, M. D., Montero, O., Gijón, M. A., Murphy,
R. C., & Sanchez, D. (2014). Schwann cell-derived Apolipoprotein D controls the dynamics of post-injury myelin recognition and degrada- tion. *Frontiers in Cellular Neuroscience*, *8*, 374.

Ghosh-Roy, A., Wu, Z., Goncharov, A., Jin, Y., & Chisholm, A. D. (2010). Calcium and cyclic AMP promote axonal regeneration in Caenorhabditis elegans and require DLK-1 kinase. *The Journal of Neuroscience: TheOfficial Journal of the Society for Neuroscience*, *30*(9), 3175–3183.

Goodrum, J. F., Earnhardt, T., Goines, N., & Bouldin, T. W. (1994). Fate of myelin lipids during degeneration and regeneration of peripheral nerve: An autoradiographic study. *The Journal of Neuroscience: The Official Journal of the Society for Neuroscience*, *14*(1), 357–367.

Gumy, L. F., Tan, C. L., & Fawcett, J. W. (2010). The role of local protein synthesis and degradation in axon regeneration. *Experimental Neurol- ogy*, *223*(1), 28–37.

Höke, A. (2006). Mechanisms of disease: What factors limit the success of peripheral nerve regeneration in humans? *Nature Clinical Practice Neurology*, *2*(8), 448–454.

Hur, E. M., & Saijilafu, Zhou, F. Q. (2012). Growing the growth cone: Remodeling the cytoskeleton to promote axon regeneration. *Trends in Neurosciences*, *35*(3), 164–174.

Jessen, K. R., Mirsky, R., & Lloyd, A. C. (2015). Schwann cells: Developmentand role in nerve repair. *Cold Spring Harbor Perspectives in Biology*, *7*(7), a020487.

Jiménez, C. R., Stam, F. J., Li, K. W., Gouwenberg, Y., Hornshaw, M. P., De Winter, F., … Smit, A. B. (2005). Proteomics of the injured rat sciatic nerve reveals protein expression dynamics during regeneration. *Molecular & Cellular Proteomics*, *4*(2), 120–132.

Kiryu-Seo, S., & Kiyama, H. (2011). The nuclear events guiding successfulnerve regeneration. *Frontiers in Molecular Neuroscience*, *4*, 53.

Kubo, T., Yamashita, T., Yamaguchi, A., Hosokawa, K., & Tohyama, M. (2002). Analysis of genes induced in peripheral nerve after axotomy using cDNA microarrays. *Journal of Neurochemistry*, *82*(5), 1129–1136. Lanza, C., Raimondo, S., Vergani, L., Catena, N., Sénès, F., Tos, P., & Geuna, S. (2012). Expression of antioxidant molecules after peripheral nerve injury and regeneration. *Journal of Neuroscience Research*, *90*(4),
842–848.

Lim, T. K., Rone, M. B., Lee, S., Antel, J. P., & Zhang, J. (2015). Mitochondrial and bioenergetic dysfunction in trauma-induced painful peripheral neuropathy. *Molecular Pain*, *11*, 58.

Ma, T. C., & Willis, D. E. (2015). What makes a RAG regeneration associated?. *Frontiers in Molecular Neuroscience*, *8*, 43.

Man, L. L., Liu, F., Wang, Y. J., Song, H. H., Xu, H. B., Zhu, Z. W., … Wang,
Y. J. (2015). The HMGB1 signaling pathway activates the inflammatory response in Schwann cells. *Neural Regeneration Research*, *10*(10), 1706–1712.

Mikol, D. D., Scherer, S. S., Duckett, S. J., Hong, H. L., & Feldman, E. L. (2002). Schwann cell caveolin-1 expression increases during myelina- tion and decreases after axotomy. *Glia*, *38*(3), 191–199.

Parikshak, N. N., Gandal, M. J., & Geschwind, D. H. (2015). Systems biology and gene networks in neurodevelopmental and neurodegenerative disorders.

Nature Reviews. Genetics, *16*(8), 441–458.

Previtali, S. C., Malaguti, M. C., Riva, N., Scarlato, M., Dacci, P., Dina, G., … Quattrini, A. (2008). The extracellular matrix affects axonal regenera- tion in peripheral neuropathies. *Neurology*, *71*(5), 322–331.

Qiu, J., Cai, D., Dai, H., McAtee, M., Hoffman, P. N., Bregman, B. S., & Filbin, M. T. (2002). Spinal axon regeneration induced by elevation of cyclicAMP. *Neuron*, *34*(6), 895–903.

Raivich, G., Bohatschek, M., Da Costa, C., Iwata, O., Galiano, M., Hristova, M., … Behrens, A. (2004). The AP-1 transcription factor c-Jun is required for efficient axonal regeneration. *Neuron*, *43*(1), 57–67.

Rishal, I., & Fainzilber, M. (2014). Axon-soma communication in neuronalinjury. *Nature Reviews Neuroscience*, *15*(1), 32–42.

Snider, W. D., Zhou, F. Q., Zhong, J., & Markus, A. (2002). Signaling thepathway to regeneration. *Neuron*, *35*(1), 13–16.

Stoll, G., Jander, S., & Myers, R. R. (2002). Degeneration and regeneration of the peripheral nervous system: From Augustus Waller's observations to neuroinflammation. *Journal of the Peripheral Nervous System*, *7*(1), 13–27.

Twiss, J. L., Kalinski, A. L., Sachdeva, R., & Houle, J. D. (2016). Intra-axonal protein synthesis−a new target for neural repair? *Neural Regeneration Research*, *11*(9), 1365–1367.

Vergara, D., Stanca, E., Guerra, F., Priore, P., Gaballo, A., Franck, J., … Maffia, M. (2017). *β*-catenin knockdown affects mitochondrial biogen- esis and lipid metabolism in breast cancer cells. *Frontiers in Physiology*, *8*, 544.

Weiss, T., Taschner-Mandl, S., Bileck, A., Slany, A., Kromp, F., Rifatbegovic, F., … Ambros, I. M. (2016). Proteomics and transcriptomics of peripheral nerve tissue and cells unravel new aspects of the human Schwann cell repair phenotype. *Glia*, *64*(12), 2133–2153.

Yi, S., Zhang, H., Gong, L., Wu, J., Zha, G., Zhou, S., … Yu, B. (2015). Deep sequencing and bioinformatic analysis of lesioned sciatic nerves aftercrush injury. *PLoS ONE*, *10*(12), e0143491.